

# Spatial and Spatiotemporal GARCH Models - A Unified Approach

Philipp Otto

Leibniz University Hannover, Germany

Wolfgang Schmid

European University Viadrina, Frankfurt (Oder), Germany

September 5, 2022

## Abstract

In time-series analyses and particularly in finance, generalised autoregressive conditional heteroscedasticity (GARCH) models are widely applied statistical tools for modelling volatility clusters (i.e. periods of increased or decreased risks). In contrast, the spatial dependence in conditional second moments of spatial and spatiotemporal processes has been considered rather uncritical until now. Only a few models have been proposed for modelling local clusters of increased risks. In this paper, we introduce a unified spatial and spatiotemporal GARCH-type model, which covers all previously proposed spatial autoregressive conditional heteroscedasticity (ARCH) models but also introduces novel spatial GARCH (spGARCH) and E-GARCH processes. For this common modelling framework, maximum-likelihood estimators are derived. In addition to the theoretical contributions, we suggest a model selection strategy verified by a series of Monte Carlo simulation studies. Eventually, the use of the unified model is demonstrated by an empirical example. In particular, we focus on real-estate prices from 1995 to 2014 in all Berlin ZIP-code areas. For these data, a spatial autoregressive model has been applied, which shows locally varying model uncertainties captured by the spatial GARCH-type models.

*Keywords:* Exponential GARCH, spatial GARCH, spatiotemporal statistics, unified approach, variance clusters, real-estate prices.

# 1 Introduction

Recently, some papers have dealt with the extension of generalised autoregressive conditional heteroscedasticity (GARCH) models to spatial and spatiotemporal processes (e.g. Otto et al. 2016, 2018, 2019; Sato and Matsuda 2017, 2018a,b). Whereas the classical ARCH model is defined as a process over time, these processes use multidimensional support. Thus, these models allow for spatially dependent second-order moments, while the local means are uncorrelated and constant in space (see Otto et al. 2019). However, direct extensions of GARCH and exponential GARCH (E-GARCH) processes to spatial settings do not exist. However, Sato and Matsuda (2017, 2018b) introduced a random process incorporating elements of GARCH and E-GARCH processes, which is neither a GARCH nor an E-GARCH process. Moreover, Otto et al. 2016 only focused on spatial ARCH processes without considering the influences from the realised, conditional variance at neighbouring locations. Thus, we introduce a novel unified spatial GARCH (spGARCH) model, which covers all previously proposed models and introduces a spGARCH and E-GARCH process for the first time. For all these models, we propose a common estimation procedure based on the maximum-likelihood approach. From a practical perspective, this unified spatial GARCH model can be used to model spill-over effects in the conditional variances. That means that an increasing variance in a certain region of the considered space would lead to an increase or decrease in the adjacent regions, depending on the direction (sign) of the spatial dependence. Local climate risks, such as fluctuations in the temperature, precipitation, and so on, or financial risks in spatially constrained markets, such as the real-estate or labour market, could be modelled using this approach. Furthermore, spatial GARCH-type models can be used as error models for any linear or nonlinear spatial regression model to account for local model uncertainties (i.e. areas where the considered models perform worse than in the remaining areas). Such model uncertainties can also be considered a kind of local risk. The remainder of the paper is structured as follows. In the following section, we introduce spatial GARCH-type models and the unified approach. Moreover, we discuss several examples of spatial GARCH-type processes including both new models. In the ensuing section, the estimation procedure is briefly described. These theoretical sections are followed by a section where we discuss the insight gained from simulation studies and a section on a real-world example. We model spatial interactions in the real-estate prices in the German capital of Berlin. In Section 5, we stress some important extensions for future research and

conclude the paper. In addition to providing all proofs, we discuss further theoretical results on the moments of the process in the Appendix.

## 2 Spatial and Spatiotemporal GARCH-Type Models

Let  $\{Y(\mathbf{s}) \in \mathbb{R} : \mathbf{s} \in D_{\mathbf{s}}\}$  be a univariate stochastic process, where  $D_{\mathbf{s}}$  is a set of possible locations in a multidimensional space. For instance,  $D_{\mathbf{s}}$  can be a subset of the  $q$ -dimensional set of real numbers  $\mathbb{R}^q$ , the  $q$ -dimensional set of integers  $\mathbb{Z}^q$ , or the Cartesian product  $\mathbb{R}^v \times \mathbb{Z}^l$ , where  $v + l = q$ . This fairly general definition of  $D_{\mathbf{s}}$  allows many spatial and spatiotemporal settings. For instance, a continuous spatial process is present in the first case, if a  $q$ -dimensional rectangle of positive volume exists in  $D_{\mathbf{s}}$  (cf. Cressie and Wikle 2011). Using this definition, spatial or spatiotemporal point processes can be modelled. Typical examples are air pollution and ozone measurements in the atmosphere. In the second case, the resulting process is a spatial lattice process mostly used for simulations and raster data, such as satellite or microscope images. In addition, spatiotemporal settings can be modelled by assuming  $D_{\mathbf{s}}$  to be a subset of the  $q$ -dimensional set of integers and the product set  $\mathbb{R}^v \times \mathbb{Z}^l$ . In this case, the temporal dimension can be easily considered one of the  $q$  dimensions. Thus, a two-dimensional spatiotemporal process would lie in the three-dimensional space. Let  $\mathbf{s}_1, \dots, \mathbf{s}_n$  denote all locations, and let  $\mathbf{Y}$  be the vector of observations  $(Y(\mathbf{s}_i))_{i=1, \dots, n}$ . The commonly applied spatial autoregressive (SAR) model assumes that the conditional variance of  $Y(\mathbf{s}_i)$  depends only on the spatiotemporal weighting matrix (cf. Cressie 1993; Cressie and Wikle 2011) but not on the observations of neighbouring locations. This approach is extended by assuming that the conditional variance can vary over space, resulting in clusters of high and low variance. By analogy to the ARCH time-series model by Engle (1982), the vector of observations is given by the nonlinear relationship

$$\mathbf{Y} = \text{diag}(\mathbf{h})^{1/2} \boldsymbol{\varepsilon} \quad (1)$$

where  $\mathbf{h} = (h(\mathbf{s}_1), \dots, h(\mathbf{s}_n))'$  and  $\boldsymbol{\varepsilon} = (\varepsilon(\mathbf{s}_1), \dots, \varepsilon(\mathbf{s}_n))'$  is a noise component, which is later specified in more detail.

## 2.1 A Unified Approach

For the unified approach, we assume that a known function  $f$  exists, which relates  $\mathbf{h}$  to a vector  $\mathbf{X} = (f(h(\mathbf{s}_1)), \dots, f(h(\mathbf{s}_n)))'$ . For the spatial and spatiotemporal GARCH-type models, this vector  $\mathbf{X}$  can be specified as

$$\mathbf{X} = \boldsymbol{\alpha} + \mathbf{W}_1 \mathbf{g}(\boldsymbol{\varepsilon}) + \mathbf{W}_2 \mathbf{X} \quad (2)$$

with a measurable function  $\mathbf{g}(\boldsymbol{\varepsilon}) = (g_1(\boldsymbol{\varepsilon}), \dots, g_n(\boldsymbol{\varepsilon}))'$ . The weighting matrices  $\mathbf{W}_1 = (w_{1,ij})_{i,j=1,\dots,n}$  and  $\mathbf{W}_2 = (w_{2,ij})_{i,j=1,\dots,n}$  are assumed to be non-negative with zeros on the diagonal (i.e.  $w_{ij} \geq 0$  and  $w_{ii} = 0$  for all  $i, j = 1, \dots, n$ ). Moreover,  $\boldsymbol{\alpha} = (\alpha_i)_{i=1,\dots,n}$  defines the level of unconditional variance, where  $\alpha_i > 0$  for  $i = 1, \dots, n$ . The existence of the inverse function of  $f$  guarantees that we can associate directly each  $\mathbf{X}$  to  $\mathbf{h}$  and vice versa. Thus, the process is real-valued and well-defined if the conditions of Theorem 1 are fulfilled.

**Theorem 1.** *Let  $\mathbf{X} = (X_i)_{i=1,\dots,n}$ . Suppose that  $\text{rk}(\mathbf{I} - \mathbf{W}_2) = n$  and that  $f : (0, \infty) \rightarrow \mathbb{R}$  has an inverse function, then Equations (1) and (2) have exactly one real-valued solution  $\mathbf{Y}$  given by  $Y(\mathbf{s}_i) = \sqrt{f^{-1}(X_i)} \varepsilon(\mathbf{s}_i)$  for  $i = 1, \dots, n$ .*

To ensure that an inverse function  $f^{-1}$  exists, it is sufficient to assume that  $f$  is a continuous and strictly increasing function on  $(0, \infty)$ . If  $f$  is unknown, it could also be estimated using a nonparametric function estimator, such as kernel estimators or splines. However, in this work, we always assume that  $f$  is known. The case of an unknown function  $f$  will be the subject of a future paper. Furthermore, spatial GARCH processes of this type are strictly stationary, if the errors  $\boldsymbol{\varepsilon}$  are strictly stationary.

**Corollary 1.** *Suppose that the assumptions of Theorem 1 are fulfilled and that  $f^{-1}$  is a measurable function. If  $(\varepsilon(\mathbf{s}_1), \dots, \varepsilon(\mathbf{s}_n))'$  is strictly stationary, then  $(Y(\mathbf{s}_1), \dots, Y(\mathbf{s}_n))'$  is strictly stationary as well.*

This unified representation allows us to model a large range of GARCH-type models with symmetric and asymmetric dependence in the conditional variances. Depending on the definition of  $f$  and  $\mathbf{g}$ , the resulting spatial GARCH-type models have different properties; thus, they are suitable for different empirical applications. In the next sections, we discuss the choices of  $f$  and  $\mathbf{g}$  for the above-mentioned spatial ARCH model (cf. Otto et al. 2018) and GARCH-like models (cf. Sato and Matsuda 2017, 2018a) as well as the novel spatial equivalent of the

GARCH model introduced by Bollerslev (1986), the exponential GARCH model by Nelson (1991), and the log-GARCH models (cf. Pantula 1986; Geweke 1986; Milhøj 1987). For some of these spatial GARCH-type models, the determination of  $\mathbf{g}(\boldsymbol{\varepsilon})$  is not straightforward. In these cases, it is easier to replace  $\mathbf{g}(\boldsymbol{\varepsilon})$  in (2) with  $\boldsymbol{\gamma}(\mathbf{Y}) = (\gamma_1(\mathbf{Y}), \dots, \gamma_n(\mathbf{Y}))'$ . It is worth noting that both approaches are equivalent if the process is invertible.

### 2.1.1 Example 1: Spatial ARCH and GARCH processes

Otto et al. (2016, 2018, 2019) assumed that

$$\mathbf{h} = \boldsymbol{\alpha} + \mathbf{W}_1 \cdot \mathbf{Y}^{(2)}, \quad (3)$$

where  $\mathbf{Y}^{(2)} = (Y(\mathbf{s}_1)^2, \dots, Y(\mathbf{s}_n)^2)'$ . This model results from the unified approach, if  $f(x) = x$ ,  $\gamma_i(\mathbf{Y}) = Y(\mathbf{s}_i)^2$ , and  $\mathbf{W}_2$  is a zero matrix. This model is the direct extension of the ARCH process by Engle (1982) to spatial and spatiotemporal processes. Otto et al. (2018, 2019) analysed this model in detail. They showed under what conditions the process is strictly stationary and determined the conditional and unconditional moments. They proved that if the matrix  $\mathbf{W}_1$  is an upper diagonal or a lower diagonal matrix (i.e. the process is oriented), then the conditional variance of the process is equal to  $h(\mathbf{s}_i)$  (i.e. the variance knowing the observations of all surrounding stations is equal to  $h$ ). Thus, this quantity has the same interpretation as in the time domain, which makes the model quite attractive. However, in the case of an arbitrary weight matrix, this assumption is no longer satisfied. They considered the situation in which  $\mathbf{W}$  also depends on an additional parameter and discussed the choice of the weight matrix. They showed that the maximum-likelihood estimators are asymptotically normally distributed for directed processes. Indeed, the spatial ARCH process can be easily extended to a spGARCH process by considering the realised values of  $h(\cdot)$  in adjacent locations. This leads to

$$\mathbf{h} = \boldsymbol{\alpha} + \mathbf{W}_1 \cdot \boldsymbol{\gamma}(\mathbf{Y}) + \mathbf{W}_2 \mathbf{h}. \quad (4)$$

Note that we refer to this particular model as spGARCH, whereas spatial GARCH-type models cover spGARCH, spatial E-GARCH and log-GARCH models as well as further approaches for modelling conditional heteroscedasticity in space. Because

$$\begin{aligned} \mathbf{h} &= \boldsymbol{\alpha} + \mathbf{W}_1 \cdot \boldsymbol{\gamma}(\mathbf{Y}) + \mathbf{W}_2 \mathbf{h} \\ &= \boldsymbol{\alpha} + \mathbf{W}_1 \cdot \text{diag}(\boldsymbol{\varepsilon}^{(2)}) \cdot \mathbf{h} + \mathbf{W}_2 \mathbf{h}, \end{aligned}$$

it holds that

$$\mathbf{h} = (\mathbf{I} - \mathbf{W}_1 \text{diag}(\boldsymbol{\varepsilon}^{(2)}) - \mathbf{W}_2)^{-1} \boldsymbol{\alpha}, \quad (5)$$

if the inverse exists. Consequently,

$$\boldsymbol{\gamma}(\mathbf{Y}) = \mathbf{Y}^{(2)} = \text{diag}(\boldsymbol{\varepsilon}^{(2)}) \mathbf{h} = \text{diag}(\boldsymbol{\varepsilon}^{(2)}) (\mathbf{I} - \mathbf{W}_1 \text{diag}(\boldsymbol{\varepsilon}^{(2)}) - \mathbf{W}_2)^{-1} \boldsymbol{\alpha} = \mathbf{g}(\boldsymbol{\varepsilon})$$

, where  $\boldsymbol{\varepsilon}^{(2)} = (\varepsilon(\mathbf{s}_1)^2, \dots, \varepsilon(\mathbf{s}_n)^2)'$ .

### 2.1.2 Example 2: Spatial E-GARCH process

The following second example provides a completely new class of spatial GARCH-type models, namely exponential GARCH models for spatial and spatiotemporal data by analogy to the E-GARCH model by Nelson (1991). The aim of the E-GARCH model is to describe asymmetries in a return process. This is caused by the leverage effect (i.e. an investor reacts differently to negative and positive news; see e.g. Day and Lewis 1992; Engle and Ng 1993; Heynen et al. 1994). Such behaviour may also arise in spatial settings. For the spatial E-GARCH process, we choose  $f(x) = \log(x)$  and  $g_i(\boldsymbol{\varepsilon}) = g(\varepsilon(\mathbf{s}_i))$  for all  $i$  with a known function  $g$ , which may depend on further parameters. Classically,  $g$  is

$$g(\varepsilon) = \Theta \varepsilon + \zeta (|\varepsilon| - E(|\varepsilon|))$$

to allow for differently weighted symmetric and asymmetric effects. Thus, the  $i$ -th component of  $\mathbf{X}$  is given by

$$\log(h(\mathbf{s}_i)) = \alpha_i + \sum_{j=1}^n w_{1,ij} g(\varepsilon(\mathbf{s}_j)) + \sum_{j=1}^n w_{2,ij} \log(h(\mathbf{s}_j)). \quad (6)$$

Further, (6) shows that

$$h(\mathbf{s}_i) = \exp(\alpha_i) \left( \prod_{j=1}^n h(\mathbf{s}_j)^{w_{2,ij}} \right) \left( \prod_{j=1}^n \exp(w_{1,ij} g(\varepsilon(\mathbf{s}_j))) \right), \quad i = 1, \dots, n. \quad (7)$$

Because of taking the logarithms, the process shows multiplicative dynamics while it possesses additive dynamics in the case of an spGARCH process (cf. Francq and Zakoian 2011). Now,  $h(\mathbf{s}_i) = Y(\mathbf{s}_i)^2 / \varepsilon(\mathbf{s}_i)^2$ . Thus,  $\log(h(\mathbf{s}_i)) = \log(Y(\mathbf{s}_i)^2) - \log(\varepsilon(\mathbf{s}_i)^2)$  (i.e.  $\mathbf{X} = \mathbf{Y}_L^{(2)} - \boldsymbol{\varepsilon}_L^{(2)}$ , where  $\mathbf{Y}_L^{(2)} = (\log(Y(\mathbf{s}_1)^2, \dots, \log(Y(\mathbf{s}_n)^2))'$  and  $\boldsymbol{\varepsilon}_L^{(2)} = (\log(\varepsilon(\mathbf{s}_1)^2, \dots, \log(\varepsilon(\mathbf{s}_n)^2))'$ , respectively). Inserting this into (6) leads to

$$(\mathbf{I} - \mathbf{W}_2) \mathbf{Y}_L^{(2)} - \boldsymbol{\alpha} = \mathbf{W}_1 \mathbf{G} + (\mathbf{I} - \mathbf{W}_2) \boldsymbol{\varepsilon}_L^{(2)}, \quad (8)$$

where  $\mathbf{G} = (g(\varepsilon(\mathbf{s}_1)), \dots, g(\varepsilon(\mathbf{s}_n)))'$ . Thus, the right side of (8) is a function of  $\boldsymbol{\varepsilon}$ , say  $f(\boldsymbol{\varepsilon})$ . Suppose that  $f$  is invertible. Then, we obtain

$$\boldsymbol{\varepsilon} = f^{-1}((\mathbf{I} - \mathbf{W}_2)\mathbf{Y}_L^{(2)} - \boldsymbol{\alpha}) \quad (9)$$

and  $\gamma_i(\mathbf{Y}) = g(\varepsilon(\mathbf{s}_i))$ .

### 2.1.3 Example 3: Hybrid spatial GARCH process

Sato and Matsuda (2017, 2018a,b) considered a slightly different choice of  $\mathbf{h}$ . They proposed choosing

$$\log(h(\mathbf{s}_i)) = \alpha_i + \sum_{j=1}^n w_{1,ij} \log(Y(\mathbf{s}_j)^2) + \sum_{j=1}^n w_{2,ij} \log(h(\mathbf{s}_j)), \quad i = 1, \dots, n. \quad (10)$$

This model can be considered a hybrid model. It uses GARCH and E-GARCH attempts (i.e.  $f(x) = \log(x)$  and  $\gamma_i(\mathbf{Y}) = \log(Y(\mathbf{s}_i)^2)$ ). However, it is neither a GARCH nor an E-GARCH process, even for one-dimensional support, where  $q = 1$ , corresponding to temporal processes. The authors use the log-transformation to avoid any non-negativity problems of  $\mathbf{h}$ , which arise in the spGARCH model. Using the notations from the previous section, (10) can be rewritten as

$$\mathbf{X} = \boldsymbol{\alpha} + \mathbf{W}_1 \mathbf{Y}_L^{(2)} + \mathbf{W}_2 \mathbf{X}. \quad (11)$$

Because  $Y(\mathbf{s}_i)^2 = h(\mathbf{s}_i)\varepsilon(\mathbf{s}_i)^2$ , it holds that  $\mathbf{Y}_L^{(2)} = \mathbf{X} + \boldsymbol{\varepsilon}_L^{(2)}$ . Now, it follows that

$$\mathbf{X} = \boldsymbol{\alpha} + (\mathbf{W}_1 + \mathbf{W}_2)\mathbf{X} + \mathbf{W}_1 \boldsymbol{\varepsilon}_L^{(2)}$$

and

$$\mathbf{X} = (\mathbf{I} - \mathbf{W}_1 - \mathbf{W}_2)^{-1}(\boldsymbol{\alpha} + \mathbf{W}_1 \boldsymbol{\varepsilon}_L^{(2)}). \quad (12)$$

Consequently,

$$\mathbf{g}(\boldsymbol{\varepsilon}) = \mathbf{X} + \boldsymbol{\varepsilon}_L^{(2)} = (\mathbf{I} - \mathbf{W}_1 - \mathbf{W}_2)^{-1}\boldsymbol{\alpha} + (\mathbf{I} + (\mathbf{I} - \mathbf{W}_1 - \mathbf{W}_2)^{-1}\mathbf{W}_1)\boldsymbol{\varepsilon}_L^{(2)}.$$

### 2.1.4 Example 4: Spatial log-GARCH process

A spatial log-GARCH process can be defined analogously to the log-GARCH process by Pantula (1986); Geweke (1986); Milhøj (1987) by choosing

$$f(x) = \log(x) \quad \text{and} \quad g(\varepsilon(\mathbf{s}_i)) = \log(|\varepsilon(\mathbf{s}_i)|^b),$$

where  $b > 0$ . In this case, an explicit solution of (9) exists because

$$\mathbf{X} = (\mathbf{I} + 0.5b\mathbf{W}_1 - \mathbf{W}_2)^{-1}(\boldsymbol{\alpha} + b\mathbf{W}_1\tilde{\mathbf{Y}}_L),$$

where  $\tilde{\mathbf{Y}}_L = (\log(|Y(\mathbf{s}_1)|), \dots, \log(|Y(\mathbf{s}_n)|))'$ . It is important to note that the hybrid model collapses to the spatial log-GARCH model, if the structures of the weighting matrices  $\mathbf{W}_1$  and  $\mathbf{W}_2$  are identical. Classically, it is assumed that  $\mathbf{W}_1 = \rho\mathbf{W}_1^*$  and  $\mathbf{W}_2 = \lambda\mathbf{W}_2^*$  with the predefined, known matrices  $\mathbf{W}_1^*$  and  $\mathbf{W}_2^*$ . In this case, there is a nonlinear dependence between  $\rho$  and  $\lambda$ , ensuring that  $\det(\mathbf{I} + 0.5\rho b\mathbf{W}_1 - \lambda\mathbf{W}_2) \neq 0$  (cf. Elhorst et al. 2012). Finally, we provide a brief overview of the considered spatial GARCH-type models and the function associated with these models in Table 1. Besides the novel models, we also show how the functions must be chosen for the models introduced by Otto et al. (2016, 2018); Otto (2019); Sato and Matsuda (2017).

[Table 1 about here.]

## 2.2 Statistical Inference

To obtain parameter estimators for the unified spatial GARCH model, we derive the likelihood functions. From (2), we obtain

$$\mathbf{X} = (\mathbf{I} - \mathbf{W}_2)^{-1}(\boldsymbol{\alpha} + \mathbf{W}_1\mathbf{g}(\boldsymbol{\varepsilon})),$$

(i.e.  $f(h(\mathbf{s}_i)) = c_i + \mathbf{d}'_i\mathbf{g}(\boldsymbol{\varepsilon})$ ). If  $f$  is invertible, we obtain  $h(\mathbf{s}_i) = f^{-1}(c_i + \mathbf{d}'_i\mathbf{g}(\boldsymbol{\varepsilon}))$ ; thus,

$$Y(\mathbf{s}_i) = \varepsilon(\mathbf{s}_i)\sqrt{f^{-1}(c_i + \mathbf{d}'_i\mathbf{g}(\boldsymbol{\varepsilon}))}$$

if  $h(\mathbf{s}_i) \geq 0$ . Suppose that  $Y(\mathbf{s}_i)$  is a continuously differentiable function of  $\boldsymbol{\varepsilon}$ . The  $(i, j)$ th element  $J_{ij}$  of the Jacobian matrix  $J = \left(\frac{\partial Y(\mathbf{s}_i)}{\partial \varepsilon(\mathbf{s}_j)}\right)_{i,j=1,\dots,n}$  is given by

$$\frac{1}{2} \frac{1}{\sqrt{f^{-1}(c_i + \mathbf{d}'_i\mathbf{g}(\boldsymbol{\varepsilon}))}} \frac{1}{f'(f^{-1}(c_i + \mathbf{d}'_i\mathbf{g}(\boldsymbol{\varepsilon})))} \mathbf{d}'_i \frac{\partial \mathbf{g}(\boldsymbol{\varepsilon})}{\partial \varepsilon(\mathbf{s}_j)} \varepsilon(\mathbf{s}_i) + \sqrt{f^{-1}(c_i + \mathbf{d}'_i\mathbf{g}(\boldsymbol{\varepsilon}))} I_{\{i\}}(j).$$

The indicator function on a set  $A$  is denoted by  $I_{\{A\}}(x)$ . Following the inverse function theorem, the inverse function exists in a neighbourhood of all points, for which the determinant of the Jacobian matrix is not equal to zero. In that case, we have  $\boldsymbol{\varepsilon} = \xi(\mathbf{Y})$ . In the above considered special cases, the inverse function  $\xi$  is easily obtained. For instance, the inverse function for the spatial E-GARCH model is given in (9). For the spGARCH and the hybrid spatial GARCH

(H-GARCH) models, it holds that  $\varepsilon(\mathbf{s}_i) = Y(\mathbf{s}_i)/\sqrt{h(\mathbf{s}_i)}$ , where  $h$  is a function of  $\mathbf{Y}$  (i.e.  $\xi(\mathbf{Y}) = \mathbf{Y} \circ (1/\sqrt{h(\mathbf{s}_i)})_{i=1,\dots,n}$ ). If the inverse function exists, then the transformation rule can be applied, and it leads to the likelihood function

$$f_{\mathbf{Y}}(\mathbf{y}) = f_{\varepsilon}(\xi(\mathbf{y})) \frac{1}{\det(J(\xi(\mathbf{y})))}. \quad (13)$$

For the four examples considered above, it holds that

$$J_{ij} = \frac{1}{2} \frac{\varepsilon(\mathbf{s}_i)}{\sqrt{h(\mathbf{s}_i)}} \frac{\partial h(\mathbf{s}_i)}{\partial \varepsilon(\mathbf{s}_j)} + \sqrt{h(\mathbf{s}_i)} I_{\{i\}}(j).$$

In the Appendix, we discuss how the partial derivatives  $\frac{\partial h(\mathbf{s}_i)}{\partial \varepsilon(\mathbf{s}_j)}$  can be obtained for the above-mentioned models.

### 3 Computational Implementation and Simulation Studies

In the ensuing sections, we focus on the practical applications of all discussed spatial GARCH-type models. In particular, we discuss the computational implementation and the insight we gained from the Monte Carlo simulation studies. Eventually, all these spatial GARCH-type models are applied to a real-world example. Below, we assume that  $\mathbf{W}_1 = \rho \mathbf{W}_1^*$ ,  $\mathbf{W}_2 = \lambda \mathbf{W}_2^*$ , and  $\boldsymbol{\alpha} = \alpha \mathbf{1}$ , where  $\mathbf{W}_1^*$  and  $\mathbf{W}_2^*$  are nonstochastic spatial weight matrices with zeros on the diagonal. Moreover,  $\rho$  and  $\lambda$  are assumed to be non-negative and  $\alpha$  is a positive constant. Using (13) and assuming that  $\varepsilon_1, \dots, \varepsilon_n$  follow the same distribution  $f_{\varepsilon}$  independently, the parameters can be estimated by the maximum-likelihood approach, that is,

$$(\rho, \lambda, \alpha)' = \arg \max_{\rho \geq 0, \lambda \geq 0, \alpha > 0} \sum_{i=1}^n \log f_{\varepsilon}(\xi_i(\mathbf{y})) - \log \det(J(\xi(\mathbf{y}))).$$

Indeed, additional parameters of  $g(\varepsilon)$  can be estimated in the same way for the spatial E-GARCH and spatial log-GARCH. We computationally implemented the unified approach in the **R**-package **spGARCH** from version 0.2.0. The package provides several main functions, namely a random number generator for spatial GARCH-type models, a function for parameter estimation for both spatial GARCH-type and mixed spatial autoregressive models with spatial GARCH-type residuals. We refer to Otto (2019) for a detailed description of the package. For the models discussed above, the functions  $f$ ,  $\mathbf{g}/\boldsymbol{\gamma}$ , and the partial derivatives  $\frac{\partial h(\mathbf{s}_i)}{\partial \varepsilon(\mathbf{s}_j)}$  are

prespecified, if the type is set to `spGARCH`, `e-spGARCH`, or `log-spGARCH`. Hence, there is no need for manual implementation. Regarding the error distribution  $f_\varepsilon$ , the package implements standard normally distributed random errors for the E-GARCH, log-GARCH, and spGARCH models. In the latter case, the normal distribution is truncated if there is no permutation such that the weighting matrix is a triangular matrix. We want to compare the considered spatial GARCH-type models. How well does the spGARCH model fit the data if it follows an E-GARCH, log-GARCH or H-GARCH model in reality? What do we lose when choosing the wrong model and how different are the models from each other? For model selection, the criteria based on the maximum value of the likelihood function can be used, such as the Akaike or Schwarz information criteria. Because the Bayesian information criterion (BIC) would tend to select a rather parsimonious model, we kept the number of unknown parameters constant for all models (i.e.  $\Theta = 0.5$ ,  $\zeta = 0$ , and  $b = 2$ ) that are assumed to be known for estimation. Thus, the models can be selected directly from the attained maximum likelihood.

To evaluate the performance of this model selection procedure, we performed a simulation study on a  $20 \times 20$  spatial unit grid (i.e.  $D_s = \{s = (s_1, s_2)' \in \mathbb{Z}^2 : 1 \leq s_1, s_2 \leq 15\}$ ), resulting in  $n = 15^2 = 225$  observations. For  $m = 1000$  replications, we simulated spGARCH, spatial H-GARCH, log-GARCH, or E-GARCH processes and estimated all four models. The weighting matrices  $\mathbf{W}_1^*$  and  $\mathbf{W}_2^*$  were chosen to be row-standardised Rook's and Queen's contiguity matrices, respectively. Furthermore, the upper diagonal elements were set to zero to avoid negative values  $h(s_i)$ , which may arise while simulating spGARCH processes. Thus, the processes can be interpreted as directional spatial processes with the origin in the upper right corner. The average values of logarithmic likelihood are reported in Table 2. Moreover, the percentages of cases in which the models were selected by this procedure are given in parentheses. The correct model was selected in the majority of cases. Generally, we observe three different groups of models. While the H-GARCH and log-GARCH models lead to similar results and values of the log-likelihood, the spGARCH and E-GARCH models are different with respect to the average log-likelihood and their model fit. In contrast to a spGARCH process having additive dynamics, the spatial E-GARCH process has a multiplicative structure. Thus, spGARCH processes behave differently to spatial E-GARCH processes, and it is important that the correct model is selected. In fact, the average values of log-likelihood of the spGARCH and E-GARCH models are not similar. On the contrary, we observe similar values for the H-GARCH and log-GARCH approaches. As the hybrid model would be identical to the spatial log-GARCH process, if

$\mathbf{W}_1^* = \mathbf{W}_2^*$ , only a few links in the weighting matrix distinguish between these two models. Thus, these models are more similar than the spGARCH and E-GARCH models.

[Table 2 about here.]

For the correct models (i.e. all combinations on the diagonal of Table 2), we further analysed the performance of the estimators. The estimated coefficients are depicted by a series of boxplots in Figure 1. The true values  $\rho = 0.5$ ,  $\lambda = 0.4$ , and  $\alpha = 1$  are shown by asterisks. It is not surprising that the estimated values for the spatial H-GARCH and log-GARCH are very similar. Hence, the fitted models would be very close to a true fit, even if the wrong model was selected. For the spGARCH and spatial E-GARCH, the estimators are also unbiased, although slightly less precise. In the ensuing section, we present an empirical application, where spatial GARCH-type models are used to describe local model uncertainties. In particular, we consider real-estate prices in all postal code regions of the German capital of Berlin.

[Figure 1 about here.]

## 4 Real-World Application: Condominium Prices in Berlin

In markets that are constrained in space, one can typically expect locally varying risks. Typical examples for such markets are the real-estate or labour markets. In the first case, the prices of properties highly depend on the locations of the real estate and the prices in the surrounding locations. Similarly, the labour market is also often constrained in space due to the limited mobility of labourers. On one hand, we observe conditional mean levels varying in space, so-called spatial clusters. On the other hand, we also may expect locally varying price risks, which can be considered local volatility clusters. Indeed, the proposed spatial GARCH-type models could capture such spatial dependencies in the conditional variance. This motivates why we consider condominium prices on a fine spatial scale. In particular, we analyse the relative changes of the Box-Cox transformed prices from 1995 to 2014 in all Berlin ZIP-code regions (i.e.  $n = 190$ ). The data are depicted in the left-hand plot of Figure 2. The sample mean of these price changes is 0.8103 with a median of 0.6965. In total, the price changes range from -2.5650 to 7.3131, while we observe a spatial cluster of positive values in the north-western ZIP-code regions. In addition, we plot the row-standardised contiguity matrix  $\mathbf{W}_1^* = \mathbf{W}_2^* = \mathbf{W}^*$  on the right-hand side.

[Figure 2 about here.]

To account for the dependence in the local means, we first estimated the coefficients of a classical spatial autoregressive model (see, e.g. Lee 2004) and then fitted the spGARCH, spatial E-GARCH, and log-GARCH models to the residuals of this autoregressive model. Hence, the GARCH parameters can be interpreted as local model uncertainties of the linear spatial autoregressive model. In Table 3, we summarise the fitted parameters of the models. Since, we have chosen  $\mathbf{W}_1^* = \mathbf{W}_2^* = \mathbf{W}^*$ , the fitted log-GARCH model coincides with the hybrid model. According to the BIC, the spatial E-GARCH models fit the residual process the best. Obviously, positive spatial dependence exists in the conditional heteroscedasticity of the residuals because all parameters are positive. This implies that clusters of higher model uncertainties and, therefore, larger prediction intervals exist. Moreover, these uncertainties spill over to the neighbouring ZIP-code regions. More precisely, we would observe multiplicative dynamics of the conditional variances for the best-fitting E-GARCH attempt. Because we would not expect asymmetry effects,  $\zeta$  has been set to zero. Eventually, we report Geary's  $C$  as measure for spatial dependence of the residuals and squared residuals.

[Table 3 about here.]

## 5 Discussion and Conclusions

Recently, a few papers have introduced spatial ARCH and GARCH-type models that allow modelling an instantaneous spatial autoregressive dependence of the heteroscedasticity. In this paper, we propose a unified spatial GARCH model covering all previous approaches. Along with these spatial ARCH-type processes, we introduce a novel spGARCH and E-GARCH model. Due to the flexible definition of the model as a set of functions, we can derive a common estimation and model selection strategy for all these spatial GARCH-type models based on the maximum-likelihood principle. However, the dependence structure does not necessarily have to be interpreted in a spatial sense. Thus, we briefly discuss a further example below. The “spatial” proximity could also be defined as edges in networks. In such cases,  $\mathbf{W}_1$  and  $\mathbf{W}_2$  would be interpreted as adjacency matrices. For instance, one might consider financial returns of several stocks as a network, where only those assets are connected that were correlated at more than a certain threshold. This could lead to a financial network, as shown in Figure

3. Thus, spGARCH models can be used to analyse information, whether volatility, risk, or spill-overs from one stock to another, if they are close to each other within a certain network. In future research, the spatial GARCH attempt for modelling volatility clusters in networks should be analysed in more detail.

[Figure 3 about here.]

In the second part of the paper, we evaluated the performance of both the parameter estimation and model selection procedure using a Monte Carlo simulation study. As this unified approach is already available in the **R**-package **spGARCH**, we briefly sketched its computational implementation. Eventually, the use of the novel model is illustrated using an empirical example. More precisely, we have shown how model uncertainties can be described by an exponential spatial GARCH model. This is the reason we analysed local price changes in the real-estate market in Berlin. In this paper, we assumed that suitable functions of the unified model framework are known. Hence, it is possible to maximise certain goodness-of-fit criteria to obtain the best-fitting model. However, these functions can also be estimated by a nonparametric approach, for instance by penalised or classical B-splines. This is the subject of a forthcoming paper.

## 6 Appendix

### Proofs and Further Results on the Stochastic Properties of the Unified Approach

Initially, we provide the proofs of Theorem 1 and Corollary 1.

*Theorem 1.* The result follows with straightforward calculations.  $\square$

*Corollary 1.* Because  $(Y(\mathbf{s}_1), \dots, Y(\mathbf{s}_n))'$  is a measurable function of  $(\varepsilon(\mathbf{s}_1), \dots, \varepsilon(\mathbf{s}_n))'$ , it is strictly stationary as well.  $\square$

Further, we want to make statements on the moments of  $\mathbf{Y}$ , for which we assume that  $\varepsilon$  is sign-symmetric, that is,

$$\varepsilon \stackrel{d}{=} ((-1)^{v_1} \varepsilon(\mathbf{s}_1), \dots, (-1)^{v_n} \varepsilon(\mathbf{s}_n)) \quad \text{for all } v_1, \dots, v_n \in \{0, 1\}.$$

Let  $c_i$  denote the  $i$ -th component of the vector  $(\mathbf{I} - \mathbf{W}_2)^{-1}\boldsymbol{\alpha}$  and  $\mathbf{d}'_i$  indicates the  $i$ -th row of matrix  $(\mathbf{I} - \mathbf{W}_2)^{-1}\mathbf{W}_1$ . Then,  $f(h(\mathbf{s}_i)) = c_i + \mathbf{d}'_i \mathbf{g}(\boldsymbol{\varepsilon})$ .

**Theorem 2.** Let  $i \in \{1, \dots, n\}$ . Suppose that the assumptions of Theorem 1 are satisfied.

- a) Let  $k \in \mathbb{N}$ . Suppose that  $f^{-1}$  is a convex function. If the  $2k$ th moments of  $\boldsymbol{\varepsilon}$  exist and  $E((f^{-1}(2\mathbf{d}'_i \mathbf{g}(\boldsymbol{\varepsilon})))^{2k}) < \infty$ , then the  $k$  moment of  $Y(\mathbf{s}_i)$  exists.
- If  $\boldsymbol{\varepsilon}$  is sign-symmetric, then  $Y(\mathbf{s}_i)$  is a symmetric random variable. All odd moments and all conditional odd moments of  $Y(\mathbf{s}_i)$  are zero, provided that they exist.

*Theorem 2.* a) Because  $2|ab| \leq a^2 + b^2$ , it follows that

$$E(|f^{-1}(c_i + \mathbf{d}'_i \mathbf{g}(\boldsymbol{\varepsilon}))|^k |\varepsilon(\mathbf{s}_i)|^k) \leq E((f^{-1}(c_i + \mathbf{d}'_i \mathbf{g}(\boldsymbol{\varepsilon})))^{2k}) + E(\varepsilon(\mathbf{s}_i)^{2k}).$$

Now, if  $f^{-1}$  is convex, it implies that  $(f^{-1}(x))^{2k}$  is convex as well. Using the inequality of Jensen, we obtain

$$E\left(\left(f^{-1}\left(\frac{2c_i}{2} + \frac{2\mathbf{d}'_i \mathbf{g}(\boldsymbol{\varepsilon})}{2}\right)\right)^{2k}\right) \leq \frac{(f^{-1}(2c_i))^{2k}}{2} + \frac{E((f^{-1}(2\mathbf{d}'_i \mathbf{g}(\boldsymbol{\varepsilon})))^{2k})}{2}.$$

Thus, the result follows.

b) The first part follows immediately because

$$Y(\mathbf{s}_i) = \sqrt{f^{-1}(c_i + \mathbf{d}'_i \mathbf{g}(\boldsymbol{\varepsilon}))} \varepsilon(\mathbf{s}_i) \stackrel{d}{=} -\sqrt{f^{-1}(c_i + \mathbf{d}'_i \mathbf{g}(-\boldsymbol{\varepsilon}))} \varepsilon(\mathbf{s}_i) = -Y(\mathbf{s}_i).$$

Moreover,

$$(Y(\mathbf{s}_1), \dots, Y(\mathbf{s}_n))' \stackrel{d}{=} (-Y(\mathbf{s}_1), \dots, Y(\mathbf{s}_n))'.$$

Thus,  $E(Y(\mathbf{s}_1)^{2k-1}|Y(\mathbf{s}_2), \dots, Y(\mathbf{s}_n)) = E(-Y(\mathbf{s}_1)^{2k-1}|Y(\mathbf{s}_2), \dots, Y(\mathbf{s}_n))$ . Consequently, this quantity is zero.

□

## Partial Derivatives

### SpGARCH

Using (5), one can derive  $\frac{\partial h(\mathbf{s}_i)}{\partial \varepsilon(\mathbf{s}_j)}$  for the spGARCH model. To be precise, we obtain

$$\frac{\partial h(\mathbf{s}_i)}{\partial \varepsilon(\mathbf{s}_j)} = \frac{\partial(\mathbf{I} - \mathbf{W}\text{diag}(\boldsymbol{\varepsilon}^{(2)}) - \mathbf{W}^*)^{-1}\boldsymbol{\alpha}}{\partial \varepsilon(\mathbf{s}_j)}.$$

From (Harville, 2008, 8.15), it follows that

$$\frac{\partial(\mathbf{I} - \mathbf{W}\text{diag}(\boldsymbol{\varepsilon}^{(2)}) - \mathbf{W}^*)^{-1}\boldsymbol{\alpha}}{\partial\varepsilon(\mathbf{s}_j)} = 2\varepsilon(\mathbf{s}_j)(\mathbf{I} - \mathbf{W}\text{diag}(\boldsymbol{\varepsilon}^{(2)}) - \mathbf{W}^*)^{-1} \cdot (\mathbf{0}, \dots, \mathbf{0}, \mathbf{w}_j, \mathbf{0}, \dots, \mathbf{0}) (\mathbf{I} - \mathbf{W}\text{diag}(\boldsymbol{\varepsilon}^{(2)}) - \mathbf{W}^*)^{-1}\boldsymbol{\alpha},$$

where  $\mathbf{w}_j$  denotes the  $j$ -th column of  $\mathbf{W}$ .

## Hybrid Spatial GARCH

Similarly, we can derive the derivative for the spatial H-GARCH model using (12), that is,

$$\frac{\partial h(\mathbf{s}_i)}{\partial\varepsilon(\mathbf{s}_j)} = \frac{\partial \log(h(\mathbf{s}_i))}{\partial\varepsilon(\mathbf{s}_j)} h(\mathbf{s}_i),$$

where  $\frac{\partial \log(h(\mathbf{s}_i))}{\partial\varepsilon(\mathbf{s}_j)} = 2d_{ij}/\varepsilon(\mathbf{s}_j)$  and  $(\mathbf{I} - \mathbf{W} - \mathbf{W}^*)^{-1}\mathbf{W} = (d_{ij})$ .

## Exponential and Logarithmic Spatial GARCH

Finally, for the spatial E-GARCH, it holds using (8) that

$$\mathbf{Z} = (\mathbf{I} - \mathbf{W}_2)^{-1}(\mathbf{W}_1\mathbf{G} + \boldsymbol{\alpha}),$$

where  $\mathbf{G} = (g(\varepsilon(\mathbf{s}_1), \dots, g(\varepsilon(\mathbf{s}_n)))')$  and

$$\frac{\partial h(\mathbf{s}_i)}{\partial\varepsilon(\mathbf{s}_j)} = \frac{\partial \log(h(\mathbf{s}_i))}{\partial\varepsilon(\mathbf{s}_j)} h(\mathbf{s}_i) = c_{ij}g'(\varepsilon(\mathbf{s}_j))h(\mathbf{s}_i),$$

where  $(\mathbf{I} - \mathbf{W}^*)^{-1}\mathbf{W} = (c_{ij})$ .

## References

Bollerslev, T. (1986). Generalized Autoregressive Conditional Heteroskedasticity. *Journal of Econometrics*, 31(3):307–327.

Cressie, N. (1993). *Statistics for Spatial Data*. Wiley.

Cressie, N. and Wikle, C. K. (2011). *Statistics for Spatio-Temporal Data*. Wiley.

Day, T. E. and Lewis, C. M. (1992). Stock market volatility and the information content of stock index options. *Journal of Econometrics*, 52(1-2):267–287.

Elhorst, J. P., Lacombe, D. J., and Piras, G. (2012). On model specification and parameter space definitions in higher order spatial econometric models. *Regional Science and Urban Economics*, 42(1-2):211–220.

Engle, R. F. (1982). Autoregressive Conditional Heteroscedasticity with Estimates of the Variance of United Kingdom Inflation. *Econometrica: Journal of the Econometric Society*, 50(4):987–1007.

Engle, R. F. and Ng, V. K. (1993). Measuring and testing the impact of news on volatility. *The Journal of Finance*, 48(5):1749–1778.

Francq, C. and Zakoian, J.-M. (2011). *GARCH models: Structure, Statistical Inference and Financial Applications*. John Wiley & Sons.

Geweke, J. (1986). Comment on modelling the persistence of conditional variances. *Econometric Reviews*, (1):57–61.

Harville, D. A. (2008). *Matrix Algebra from a Statistician’s Perspective*, volume 1. Springer.

Heynen, R., Kemna, A., and Vorst, T. (1994). Analysis of the term structure of implied volatilities. *Journal of Financial and Quantitative Analysis*, 29(1):31–56.

Lee, L.-F. (2004). Asymptotic Distributions of Quasi-Maximum Likelihood Estimators for Spatial Autoregressive Models. *Econometrica*, 72(6):1899–1925.

Milhøj, A. (1987). *A multiplicative parameterization of ARCH models*. Universitetets statistiske Institut.

Nelson, D. B. (1991). Conditional heteroskedasticity in asset returns: A new approach. *Econometrica: Journal of the Econometric Society*, pages 347–370.

Otto, P. (2019). spGARCH: An R-package for spatial and spatiotemporal ARCH models. *to appear in: The R Journal*.

Otto, P., Schmid, W., and Garthoff, R. (2016). Generalized spatial and spatiotemporal autoregressive conditional heteroscedasticity. *arXiv:1609.00711*.

Otto, P., Schmid, W., and Garthoff, R. (2018). Generalised Spatial and Spatiotemporal Autoregressive Conditional Heteroscedasticity. *Spatial Statistics*, 26:125–145.

Otto, P., Schmid, W., and Garthoff, R. (2019). Stochastic properties of spatial and spatiotemporal arch models. *Statistical Papers*.

Pantula, S. G. (1986). Comment on modelling the persistence of conditional variances. *Econometric Reviews*, 5(1):71–74.

Sato, T. and Matsuda, Y. (2017). Spatial autoregressive conditional heteroskedasticity models. *Journal of the Japan Statistical Society*, 47(2):221–236.

Sato, T. and Matsuda, Y. (2018a). Spatial GARCH models. Technical report, Graduate School of Economics and Management, Tohoku University.

Sato, T. and Matsuda, Y. (2018b). Spatiotemporal ARCH models. Technical report, Graduate School of Economics and Management, Tohoku University.

## List of Figures

1	Boxplot of the estimated parameters for 1000 replications to illustrate the performance of the proposed estimators. The true underlying values are given by an asterisk for each parameter. . . . .	19
2	Relative changes (in per cent) of the Box-Cox transformed prices in all Berlin ZIP-code regions and the applied spatial weight matrix, which coincides with a classical row-standardised first-order contiguity matrix. . . . .	20
3	Financial network of selected stocks of the S&P 500, where the colour of the nodes denotes the annual returns in 2017, where darker colours indicate higher returns. . . . .	21

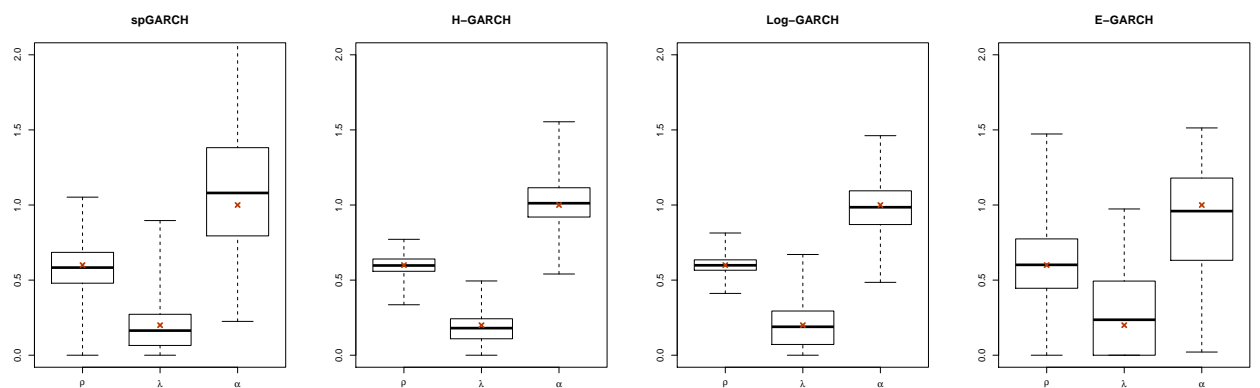


Figure 1: Boxplot of the estimated parameters for 1000 replications to illustrate the performance of the proposed estimators. The true underlying values are given by an asterisk for each parameter.

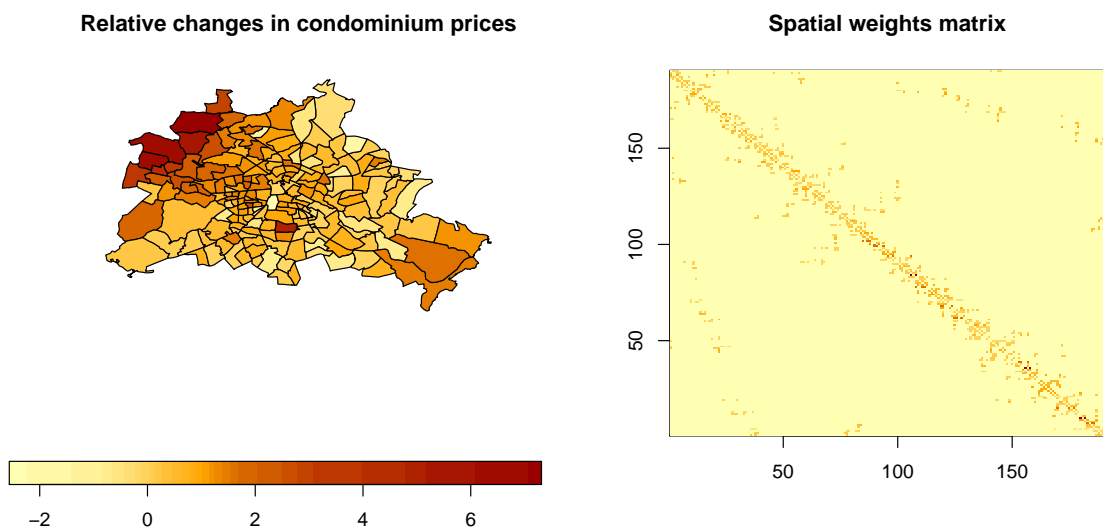


Figure 2: Relative changes (in per cent) of the Box-Cox transformed prices in all Berlin ZIP-code regions and the applied spatial weight matrix, which coincides with a classical row-standardised first-order contiguity matrix.

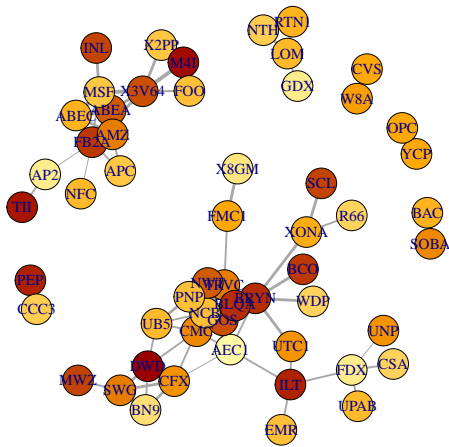


Figure 3: Financial network of selected stocks of the S&P 500, where the colour of the nodes denotes the annual returns in 2017, where darker colours indicate higher returns.

## List of Tables

1	Overview of different spatial GARCH-type models nested in the unified approach.	23
2	Average value of the logarithmic likelihood function and percentage of selections within 1000 trials per row (i.e. each model has been simulated with 1000 replications). In the rows, the simulated model is given (i.e. the true model, which should be selected by the procedure). The estimated models are given by columns. The row-wise largest average log-likelihood and percentage of selections are printed in bold. . . . .	24
3	Estimated parameters of the spGARCH model for the residuals of a spatial autoregressive model, where the dependent variables are the price changes in the condominium prices in Berlin. All standard errors are given in parentheses. . . .	25

Table 1: Overview of different spatial GARCH-type models nested in the unified approach.

Model	$f$	$\mathbf{g}/\boldsymbol{\gamma}$	$\mathbf{W}_2$
<i>New models</i>			
Spatial GARCH model	$f(x) = x$	$\gamma_i(\mathbf{Y}) = Y(\mathbf{s}_i)^2$	$\mathbf{W}_2$
Spatial E-GARCH model	$f(x) = \log(x)$	$g_i(\boldsymbol{\varepsilon}) = \Theta \varepsilon(\mathbf{s}_i) + \zeta( \varepsilon(\mathbf{s}_i)  - E( \varepsilon(\mathbf{s}_i) ))$	$\mathbf{W}_2$
Spatial log-GARCH model	$f(x) = \log(x)$	$g_i(\boldsymbol{\varepsilon}) = \log( \varepsilon(\mathbf{s}_i) ^b)$	$\mathbf{W}_2$
<i>Previously proposed models</i>			
Spatial ARCH model (Otto et al. 2016, 2018)	$f(x) = x$	$\gamma_i(\mathbf{Y}) = Y(\mathbf{s}_i)^2$	$\mathbf{0}$
Hybrid spatial GARCH model (Sato and Matsuda 2017)	$f(x) = \log(x)$	$\gamma_i(\mathbf{Y}) = Y(\mathbf{s}_i)^2$	$\mathbf{W}_2$
Spatial Log-ARCH model (Otto 2019)	$f(x) = \log(x)$	$g_i(\boldsymbol{\varepsilon}) = \log( \varepsilon(\mathbf{s}_i) ^b)$	$\mathbf{0}$

Table 2: Average value of the logarithmic likelihood function and percentage of selections within 1000 trials per row (i.e. each model has been simulated with 1000 replications). In the rows, the simulated model is given (i.e. the true model, which should be selected by the procedure). The estimated models are given by columns. The row-wise largest average log-likelihood and percentage of selections are printed in bold.

Simulated model	Estimated model						
	spGARCH	H-GARCH	Log-GARCH	E-GARCH			
spGARCH	<b>-455.722</b> (93.9%)	-463.629 (3.1%)	-464.023 (2.5%)	-474.053 (0.5%)			
H-GARCH	-472.452 (0.0%)	<b>-451.418</b> (93.7%)	-455.530 (6.3%)	-535.889 (0.0%)			
Log- GARCH	-378.353 (0.0%)	-362.973 (0.3%)	<b>-352.104</b> (99.7%)	-393.634 (0.0%)			
E-GARCH	-461.607 (3.3%)	-461.850 (2.2%)	-462.029 (2.1%)	<b>-458.491</b> (92.4%)			

Table 3: Estimated parameters of the spGARCH model for the residuals of a spatial autoregressive model, where the dependent variables are the price changes in the condominium prices in Berlin. All standard errors are given in parentheses.

Parameter	spGARCH model		Log-GARCH model		E-GARCH model	
	Estimate		Estimate		Estimate	
<i>Mean equation</i>						
$\mu$			0.2002	(0.0813)		
$\gamma$			0.7456	(0.0588)		
<i>Residuals process</i>						
$\alpha$	0.0557	(0.0350)	0.1829	(0.0667)	3.3426	(0.9484)
$\rho$	0.1768	(0.0673)	0.1235	(0.0471)	2.0086	(0.6423)
$\lambda$	0.7093	(0.1061)	0.9233	(0.0652)	2.4944	(1.0058)
$b$	-	-	2.8621	(0.6808)	-	-
$\Theta$	-	-	-	-	1.6046	(0.9687)
<i>Summary statistics</i>						
LL	-230.4026		-240.2949		-162.1902	
BIC	476.5462		501.5780		345.3685	
$C$ res. ( $p$ -value)	1.0643	(0.1817)	1.0531	(0.2951)	1.1104	(0.0171)
$C$ squ. res. ( $p$ -value)	1.0505	(0.4769)	1.0105	(0.8886)	0.9734	(0.6977)